SVU-International Journal of Engineering Sciences and Applications (2024) 5(2): 119-128
Print ISSN 2785-9967 | Online ISSN 2735-4571
DOI 10.21608/SVUSRC.2024.276737.1190

# Experimental Investigation of a Novel Thermosyphon Solar Water Heater Performance under Aswan Climate Conditions

**Mahmoud Eid El-saggan[□,1], Ahmed Rekaby[2], Walid Aniss Aissa[3], and Ahmed M. Reda[4]**

**Abstract** In numerous regions globally, Solar Water Heaters (SWHs) and Solar Lighting Pipes (SLPs) are widely adopted, contributing significantly to energy conservation. While SWHs are moderately utilized, SLPs remain largely unfamiliar in Egypt. This study introduces an innovative merged energy-saving approach that merges SWH and SLP into a unified system. The combination concept involves incorporating a solar heater via a serpentine pipe's collector, utilizing the available space surrounding the daylight gadget tube. Key objectives of this integration include cost reduction in manufacturing, enhanced solar energy savings, and minimizing space requirements. Furthermore, recent daytime power outages in Egypt, stemming from escalating consumption exceeding production capacities, have spurred this investigation. The paper presents a comprehensive analysis of the Passive-Thermosyphon performance of the proposed SWH across various seasons in Aswan, Egypt, characterized by its sunny and arid climate, to assess its practical applicability. Results indicate a successful elevation in water temperature, with the highest recorded at about 70°C and a maximum instantaneous efficiency of around 36%. Moreover, the suggested solar heater demonstrated a peak daily thermal efficiency of approximately 31% during testing.

**Keywords:** Energy efficiency; passive thermosyphon; serpentine tubes; solar heater; tubular collector.

## 1 Introduction

Due to the ongoing global population growth and the subsequent reliance on technology, electricity production has surged, reaching approximately 26,940 TWh by 2023 [1]. Notably, around 17,010 TWh, or 63.14%, of generated electricity stems from the combustion of fossil fuels, namely oil, natural gas, and coal [2]. In Egypt, fossil fuels account for approximately 90% of electricity generation [3]. This escalating demand has precipitated a notable depletion in fossil fuel reserves, with little expectation for these reserves to suffice future demands. Concurrently, carbon dioxide emissions are projected to escalate, potentially reaching around 43 billion metric tons by 2040 [4]. Consequently, there has been a recent shift towards renewable energy sources as a means to conserve energy and foster sustainable development [5–7].

Given that a vast majority of individuals spend approximately 90% of their time within residential structures [8], there is a heightened demand for electricity-intensive amenities within these buildings, including water heating, lighting, and air conditioning. Water heating, in particular, is a critical aspect, accounting for approximately 23%, 18%, 14%, and 16% of residential energy consumption in Australia, the United States, the European Union, and Egypt, respectively [9]. Similarly, lighting constitutes around 35%, 28%, 26%, and 33% of residential energy consumption in India, the United States, the European Union, and Egypt, respectively [10,11]. Consequently, the outlook for renewable energy, particularly solar energy employed for water heating and lighting, appears advantageous and is undergoing steady ripening. Notably, in developing nations such as Egypt, within the framework of the country's 2030 Sustainable Development Plan, solar energy has emerged as a competitive and economically viable energy alternative, especially following the energy subsidies cutting [12,13].

A considerable portion of the existing literature has centered on energy-efficient applications, exemplified by Solar Light Pipes (SLPs) and Solar Water Heaters (SWHs). These pipes serve as substitutes for conventional light sources, gathering sunlight from the outdoors and channeling it into enclosed spaces devoid of natural light

Received: 13 March 2024/ Accepted: 15 April 2024
□Corresponding Author: Mahmoud Eid El-saggan,
E-mail: mahmoudeid@energy.aswu.edu.eg
[1,2,3,4] Department of Mechanical Power Engineering, Faculty of Energy Engineering, Aswan University, Aswan 81528, Egypt

sources, such as enclosed corridors, warehouses, and subterranean areas, through high-reflective tubing. Among these solutions, SWHs stand out as the most prevalent and longstanding energy-saving technology. These systems leverage the thermal energy converted from sunlight striking the Flat Plate Collector (FPC) within the SWH to heat water effectively.

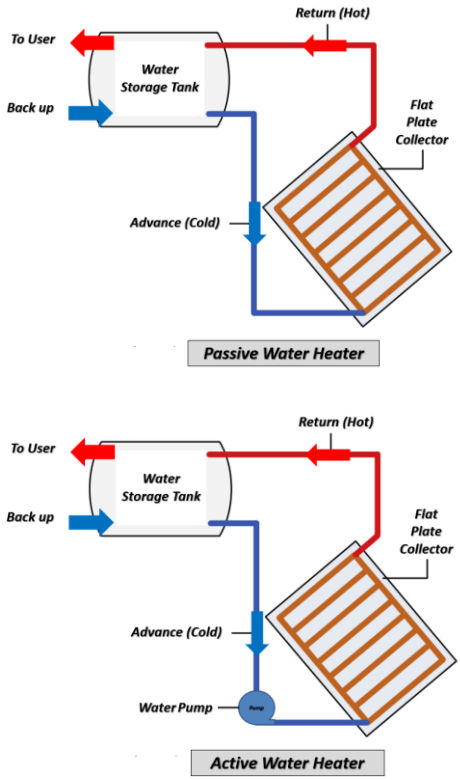


**Fig. 1.** Passive and active solar water heater systems.

Operationally, there are two approaches used, as Figure 1 illustrates: passive and active. Thermosyphon SWH and integrated storage are included in the passive method (Fig. 2). Thermosyphon SWH systems rely on natural circulation, which makes them easy to use and low-maintenance. Passive-Thermosyphon solar water heaters (SWHs) are hence the most popular kind. The key conclusions of eminent scientists in earlier theoretical and experimental investigations pertaining to SWHs are given in the paragraph that follows.

In Slama's investigation [14], a notable efficiency increase of 42% was attained through the incorporation of double glazing. Similarly, in the research conducted by Hellstrom et al. [15], the addition of an anti-reflective layer to the glass yielded compelling results. They observed that at an ambient temperature of 50°C, the enhanced solar glass transmittance by 4% contributed to a 6.5% boost in annual output. Föste et al. [16] introduced a thermochromic absorber coating with a distinctive feature: its emissivity can vary by up to 0.35 based on temperature changes. Utilizing this thermochromic absorber coating, the overall system performance saw an increase from 1.5% to 4.5% compared to conventional absorber coatings. Meanwhile, Jyothi et al. [17] developed a novel 5-layered nanostructure comprising TiAlC / TiAlCN / TiAlSiCN / TiAlSiCO / TiAlSiO for tandem absorption. This tandem absorber-reflector setup includes absorbing layers of TiAlC (titanium aluminum chloride), TiAlCN (titanium aluminum carbonitride), and TiAlSiCN (titanium aluminum silicon carbonitride), complemented by semi-transparent and anti-reflecting layers of TiAlSiCO (titanium aluminum silicon cobalt) and TiAlSiO (titanium aluminum silicon oxide). In practical application, the absorption material demonstrated stability up to 598 K in air for 400 hours and 923 K in a vacuum for 100 hours. However, tandem absorbers tend to degrade under higher temperatures due to their relatively unstable microstructure [18]. The serpentine tube collector design (Fig. 3) was introduced by Al-Matrawy and Farkas [19] to address certain drawbacks associated with the parallel design. These limitations include non-uniform temperature distribution on the absorber, uneven water distribution inside the risers, and heightened heat loss to the collector, particularly evident during low flow rate conditions [20]. Smyth [21] and Kalogirou [22] advised maintaining a maximum vertical distance of 50 cm between the top of the collector and the bottom of the storage tank to prevent thermosyphon reverse circulation, particularly noticeable during nighttime. Additionally, they suggested inclining serpentine pipes to deter the formation of air pockets, which can impede fluid flow.

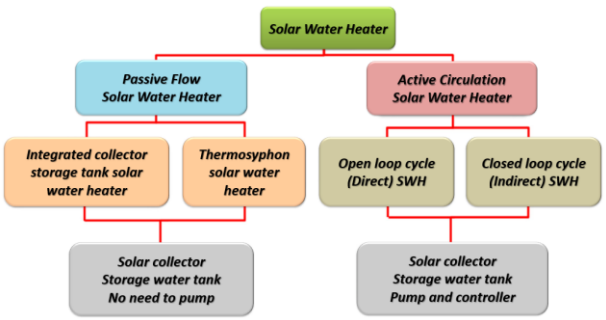


**Fig. 2.** Simplified classification chart of the solar water heater systems based on the circulation method.

A concept that helps enhance heat and efficiency in solar heaters is phase change materials (PCMs), which store thermal energy during the daytime and return it at nighttime [23]. Fig. 4 summarizes the most important results reached by some researchers as a result of using these improved materials [24-36]. In Mirzaei et al.'s study [37], it was found that $Al_2O_3$ nanofluid has good thermal characteristics, which led to a 23.6% increase in the collector efficiency. Metwally et al. [38] obtained an efficiency of 49% as a result of inserting transparent rectangular slats or strips inside the FPC. A similar study by Abene et al. [39] reported an efficiency of 50% due to the addition of obstacles inside the flat collector. In Kumar and Parsad's [40] study, the results of inserting a twisted tape (TT) within the absorber tube in a serpentine solar collector showed that the maximum improvement was found to be 18–70%. In Puthilibai et al.'s [41] study, due to utilizing the aluminum TT turbulator effect, the maximum temperature attained is 75°C.

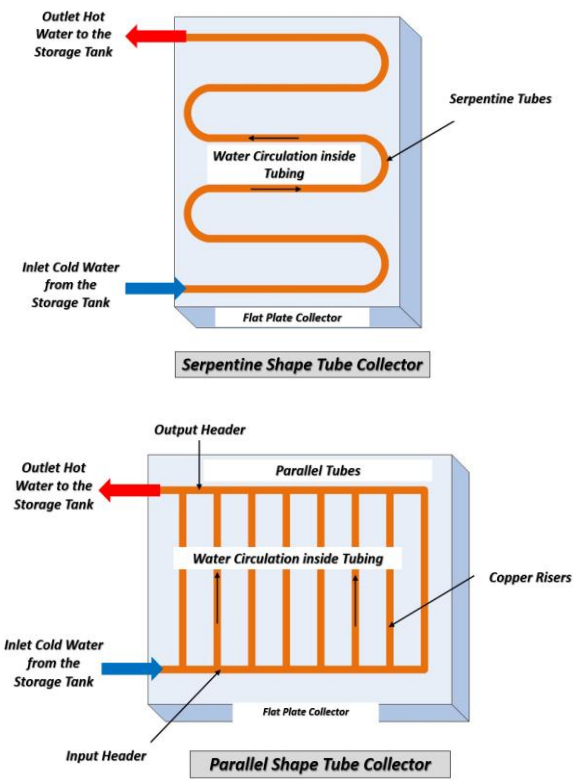


**Fig. 3.** Serpentine and parallel shape pipe collector designs.

SLP and SWH systems are widely used in many regions of the world, making it easier to conserve energy. However, SWH is not yet widely used in Egypt, and SLP is still unknown in Egypt. These separate systems require distinct production costs and occupy separate spaces. This has prompted our proposal for an integrated energy-saving system, amalgamating SLP and SWH into a consolidated model. By utilizing the vacant space surrounding the SLP perimeter, the two devices are integrated using a serpentine collector to facilitate SWH. The tubular design of the SWH introduced in this study shares similarities with customary FPCs in terms of components, albeit with modified formatting. In this paper, the Passive-Thermosyphon performance of the proposed SWH is presented and analyzed in detail across different seasons of the year in Aswan, Egypt, which has a sunny and dry climate, to evaluate its practical utility.

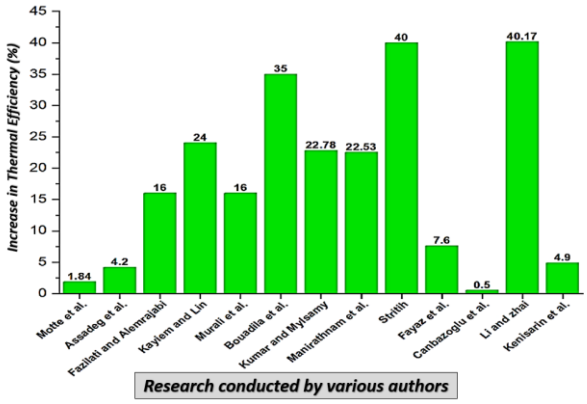


**Fig. 4.** Thermal efficiency improvement by different authors using PCMs.

## 2 Martials and Methods

The evaluation of the inventive Thermosyphon Solar Water Heater, illustrated in Figs. 5 and 6, took place at the Faculty of Energy Engineering, Aswan University, located in Aswan City, Egypt, positioned at coordinates (latitude: 24°5′N and longitude: 32°53′E).

The existing integrated system was designed to combine the passive solar light pipe with the natural solar water heater functionalities. It includes a transparent dome that captures sunlight and channels it through a highly reflective cylindrical tube to a lighting diffuser. Surrounding the solar lighting pipe is a copper TPC, insulated between layers. The exterior of the copper absorber or collector is coated with black paint to enhance solar ray absorption. Additionally, it is enveloped by a copper serpentine with a black coating and encased in double-cylindrical-glazing sheets to trap absorbed heat. Working on the Thermosyphon truth, water circulates via the integrated system.

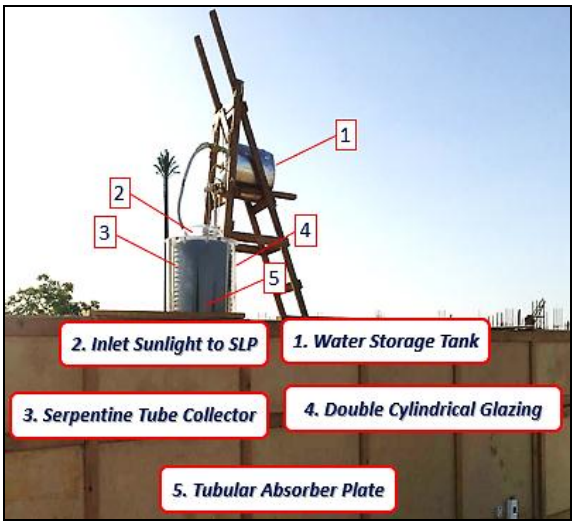


**Fig. 5.** A picture of the incorporated experiment system.

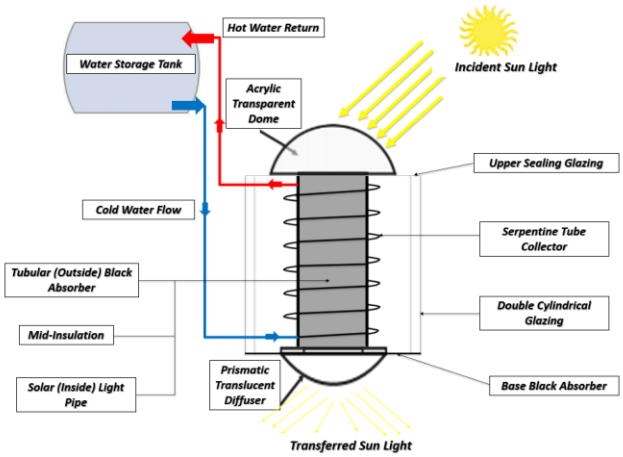


**Fig. 6.** A detailed schematic diagram showing the parts of the system under study.

## 2.1 Experimental setup

The actual dimensions of the current SWH are 0.7 m in height, 0.45 m in diameter for the tubular absorber, and 0.6 m in diameter for the double-glazing panels that surround it. The diameter and length of the tube for the SLP are 0.4 m and 0.75 m, respectively. The TPC and SLP are separated by an insulating layer that is 0.025 m thick. This prevents thermal loss from the back of the light tube and shields it from thermal and physical shocks. Thermal conductivity, k= 0.17 W. $m^{-1}.^{\circ}C^{-1}$ is achieved by using 0.0015 m transparent acrylic glass sheets (with 92% total transmissivity) for the double cylindrical glazing that is in use [42]. By acting as a transparent heat barrier, it prevents heat from escaping into the surrounding spaces. A loft glazing seal made of clear acrylic sheeting was installed on top of the SWH, facing the sky, to help transmit solar rays to the tubular collector during the sun's perpendicular peak hours of 11 a.m. to 1 p.m. It also keeps the heater's internal temperature from dropping. Because its k= 401 W. $m^{-1}.^{\circ}C^{-1}$, the serpentine design shaped pipe collector manufactured of copper with a diameter of 0.01 m was selected [43].

Furthermore, as previously indicated, the serpentine pipe collector was chosen because to its greater efficiency as compared to the parallel pipe collector. To reduce the amount of space occupied by the flat collector, the TPC is utilized in place of the FPC in the novel SWH model, along with the same other components. The newly designed solar heater just makes use of the SLP area that is already being used to illuminate interior rooms. As seen in Fig. 5, the top dome is constructed of transparent acrylic that blocks the heat entrance (i.e., infrared rays) and only permits the sunlight transference or visible light from the solar-spectrum. To optimize light transmission efficiency through the tube, the light transmission tube is constructed using 98% reflective steel sheets. To optimize solar absorptivity, black paint is also applied externally to the TPC and serpentine pipe collector (Fig. 5). Ultimately, thermal insulation and metal reflective film are used to isolate the water storage tank from the ambient temperature. In addition, the water pathways that rise and descend are isolated.

**Table 1.** Specifications of the measurement tools.

| Measuring device | Range | Uncertainty |
|---|---|---|
| Data acquisition and thermocouples [°C] | –50 to 900 | ± 0.25 |
| Pyranometer [W. $m^{-2}$] | 0 to 2000 | ± 5% |
| Thermometer [°C] | -200 to 1370 | ±(0.2%+0.6) |
| Flow meter [L. $min^{-1}$] | 0 to 6 | ± 5% |

## 2.2 Measurement tools

Four K-type thermocouples and a data acquisition system (Omega 3005) were utilized to measure the temperatures of both the storage water and the output water collector. Within the storage water tank, three thermocouples were vertically positioned, with the first placed at the top, the second in the middle, and the third at the bottom. The entry collector temperature was determined by averaging the data from these three thermocouples. Sun insolation was measured using a Kipp and Zonen kind pyranometer (model CMP3), with the data recorder connected to both the pyranometer and the thermocouples. Additionally, a digital (type UT325) thermometer and a water flow (YFS401) meter were employed to record ambient temperature and water flow

rate, respectively. Table 1 provides detailed specifications of the measurement tools utilized in the experiment.

**Table 2.** Experiments performed on the suggested SWH.

| Date | Season | Remarks |
|---|---|---|
| June 21, 2021 | Summer | ▪ The environmental conditions in the vicinity are assessed and documented, incorporating measurements of solar radiation intensity, ambient temperature, as well as the temperatures within the SWH system. ▪ The instantaneous and daily thermal efficiencies of the solar heater under examination are computed. |
| September 23, 2021 | Autumn | |
| December 21, 2021 | Winter | |
| March 22, 2022 | Spring | |

## 2.3 Experimental procedure

The experimental procedure remained consistent across all tests. Table 2 shows the days and seasons of the tests administered. The following experimental procedure was adhered to:

- The integrated system is constructed, washed, sanitized, and dried.
- System parts are interconnected and mounted on the testing facility roof.
- Subsequently, the hold water tank is loaded with 60 L of spout water.
- Surrounding temperature is observed utilizing a calibrated thermometer.
- The test is initiated by emptying water from the water-tank through the incorporated SWH and initiating circulation via the thermosyphon-effect.
- The Passive-Thermosyphon SWH operates by simply supplying water from the bottom outlet of the storage tank.
- Following this, water circulates through the TPC, absorbing incident solar radiation and converting it into thermal energy for the water within the collector pipes.
- Heated water is then directed-back to the water storage tank through the upper inlet.
- Colder inlet water, denser due to lower temperatures, settles at the bottom of the tank and is also drawn into the collector's base.
- Conversely, as the water temperature rises, less dense water ascends to the top of the tank via the outlet tube.
- Measurements are registered over eight hours of sunshine (i.e., from 8 a.m. to 4 p.m.).
- Water storage, outlet collector temperatures, and solar insolation are measured and recorded using K-type thermocouples and a pyranometer connected to a data logger (every 15 minutes and integrated over 1 hour).

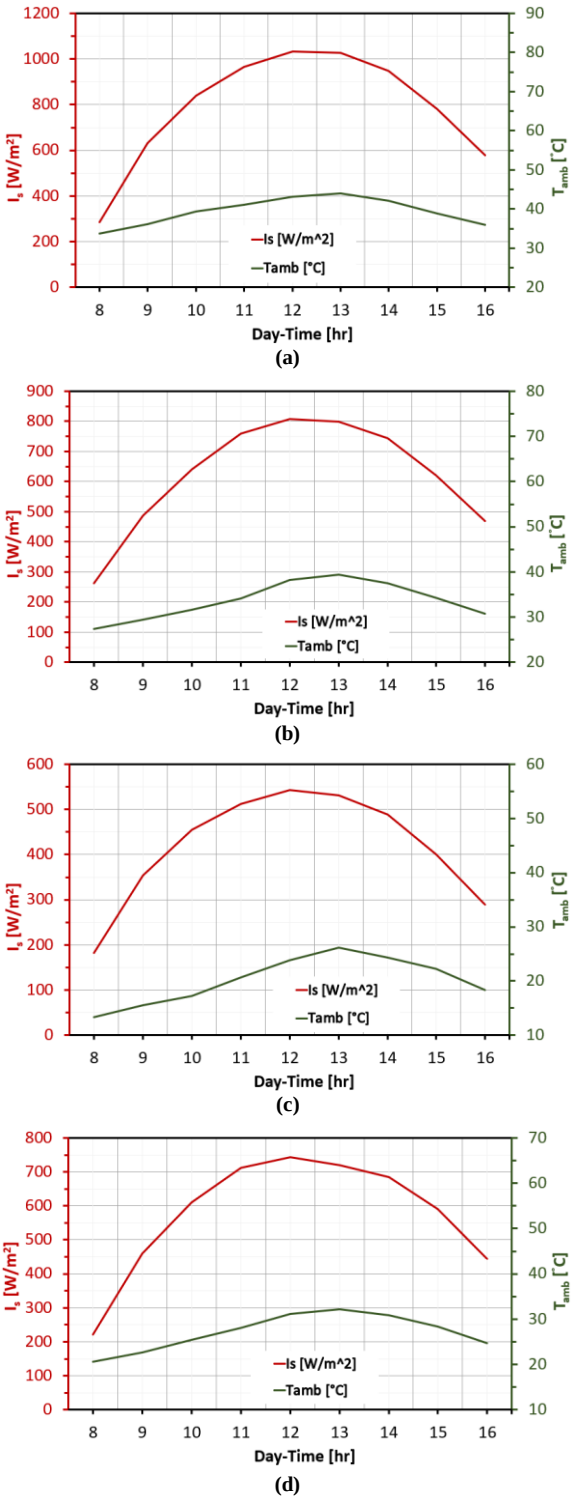


**Fig. 7.** Variation of the solar radiation intensity ($I_s$) and the ambient temperature ($T_{amb}$) through the test period for (a) June 21, 2021, (b) September 23, 2021, (c) December 21, 2021, and (d) March 22, 2022.

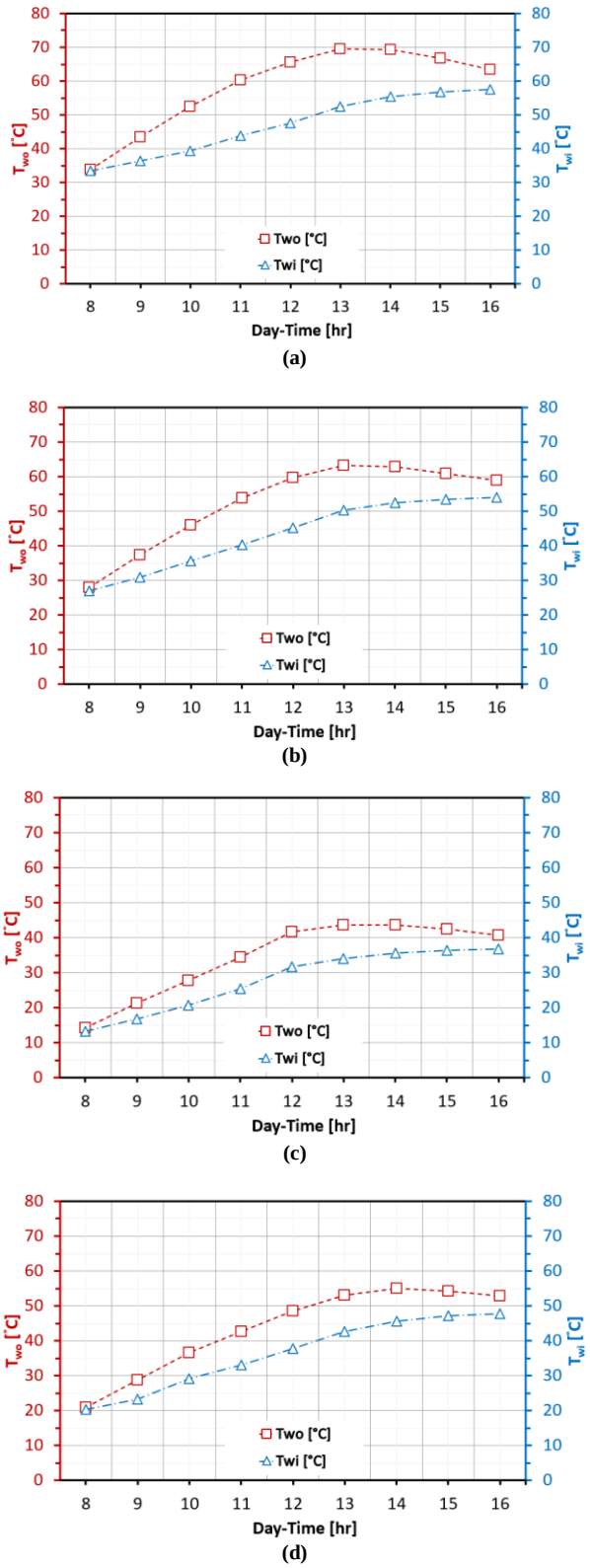


**Fig. 8.** Variance of the outlet water temperature ($T_{wo}$) and the inlet water temperature ($T_{wi}$) through the test period for (a) June 21, 2021, (b) September 23, 2021, (c) December 21, 2021, and (d) March 22, 2022.

## 2.4 Efficiency evaluation

It is necessary to look at how the sun's insolation and surrounding temperature affect the suggested solar heater's effectiveness in different seasons in order to determine how practical it is. The following equation can be used to calculate the instantaneous thermal efficiency of the heater, represented as $\eta_{th,\,ins}$ [44].

$$\eta_{th,ins} = \frac{\dot{Q}_{useful}}{\dot{Q}_{solar}} \quad (1)$$

The following formulas are used to determine the solar insolation input power and the usable output heat power.

$$\dot{Q}_u = \dot{m}_w\, C_{pw}\, (T_{wo} - T_{wi}) \quad (2)$$

$$\dot{Q}_s = I_s\, A_s \quad (3)$$

where Twi and Two are the water collector's intake and outlet temperatures in [°C], respectively, and ṁw is the water mass flow rate in [kg. s-1]. Cpw is the water specific heat in [J. kg-1. °C-1]. The incident solar radiation is expressed as Is in [W. m-2], while the collector area for solar heater or serpentine tubes is expressed as As in [m2].

Enter the following values into equations 2 and 3, replacing: (1) $\dot{m}_w$ (mass flow rate) = 0.0042 kg. $s^{-1}$ (or volume flow rate, $Q_w$= 15 L/h); (2) $C_{pw}$= 4187 J. $kg^{-1}$. $^{\circ}C^{-1}$; (3) $A_s$= N($\pi D_{abs}$)($\pi D_t$), where $D_{abs}$= 45 cm is the circular serpentine tube radius or absorber diameter, $D_t$= 1 cm is the external diameter of the copper tube, and N= 20 is the number of turns or coils. Afterwards, the thermal efficiency instantaneous, $\eta_{th,\,ins}$, will be;

$$\eta_{th,ins} = \frac{17.6\ \Delta T_w}{0.9\ I_s}\ 100\ (\%) \quad (4)$$

## 3 Results and Discussions

Aswan City's normal environmental conditions were employed for an experimental test of the TPC's efficiency in the present system. In order to assess the SWH's performance in real practical use, it was examined and studied against various temperatures and weather circumstances throughout the year, i.e., throughout various seasons of the year, as shown in the following paragraphs and Figures 7 - 9.

In 21 June 2021, being a summer month, the initial experiment was carried out on the present solar heater. During this period, the system's efficacy was evaluated by documenting the water and surrounding temperatures

alongside solar insolation levels. As depicted in Figures 7 – 9, the peak water temperature achieved during this timeframe stood at approximately 70°C. Moreover, under a total solar insolation of 7090 W/m$^2$/day and a recorded maximum surrounding temperature of 44°C, the highest instantaneous thermal efficiency reached 34.5%. Observing Figures 7 – 9, it becomes apparent that with the rise in solar radiation and the disparity between water temperatures, the ratio $\Delta T_w/I_s$ escalates, thereby augmenting the efficiency of the tubular collector until it reaches a pinnacle, followed by a subsequent decline.

In 23 September 2021, during the autumnal season, the heater under investigation was the subject of the second experiment. This period's measurements and displays of the surrounding air temperature, solar insolation, and consequent water temperature are shown in Figs. 7 and 8. Simultaneously, the performance of the current heater system was evaluated (Fig. 9). As portrayed in Figures 7 – 9, the peak water temperature achieved during this timeframe stood at 63.3°C. Moreover, under a total sun insolation of 5590 W/m$^2$/day and a recorded maximum surrounding temperature of 39.4°C, the highest instantaneous thermal efficiency reached 35.5%. Upon examining Figs. 7 - 9, it becomes evident that as solar radiation and the difference between water temperatures increase, the ratio $\Delta T_w/I_s$ also rises, leading to an increase in collector efficiency until reaching its peak, after which it gradually declines.

In 21 December 2021, a winter's day, the third test was carried out on the SWH. Together with the output water temperatures, other relevant meteorological data were recorded, such as ambient temperature and solar insolation (Figs. 7 and 8). In the interim, the water heater's efficiency for this period was also computed, as shown in Fig. 9. As depicted in Figures 7 – 9, the peak water temperature achieved during this timeframe stood at approximately 44°C. Moreover, under a total ray's exposure of 3730 W/m$^2$/day and a recorded maximum ambient temperature of about 26.5°C, the highest instantaneous efficiency reached 36.5%.

In 22 March 2022, a spring's day, the fourth experimentation was conducted on the suggested heater. Together with the output water temperatures, other relevant meteorological data were recorded, such as surrounding temperature and sun insolation (Figs. 7 and 8). In the interim, the heater's efficiency for this period was also computed, as shown in Fig. 9. As depicted in Figures 7 – 9, the peak water temperature achieved during this timeframe stood at 55°C. Moreover, under a total ray's exposure of 5190 W/m$^2$/day and a recorded maximum surrounding temperature of about 33°C, the highest instantaneous efficiency reached about 29%.

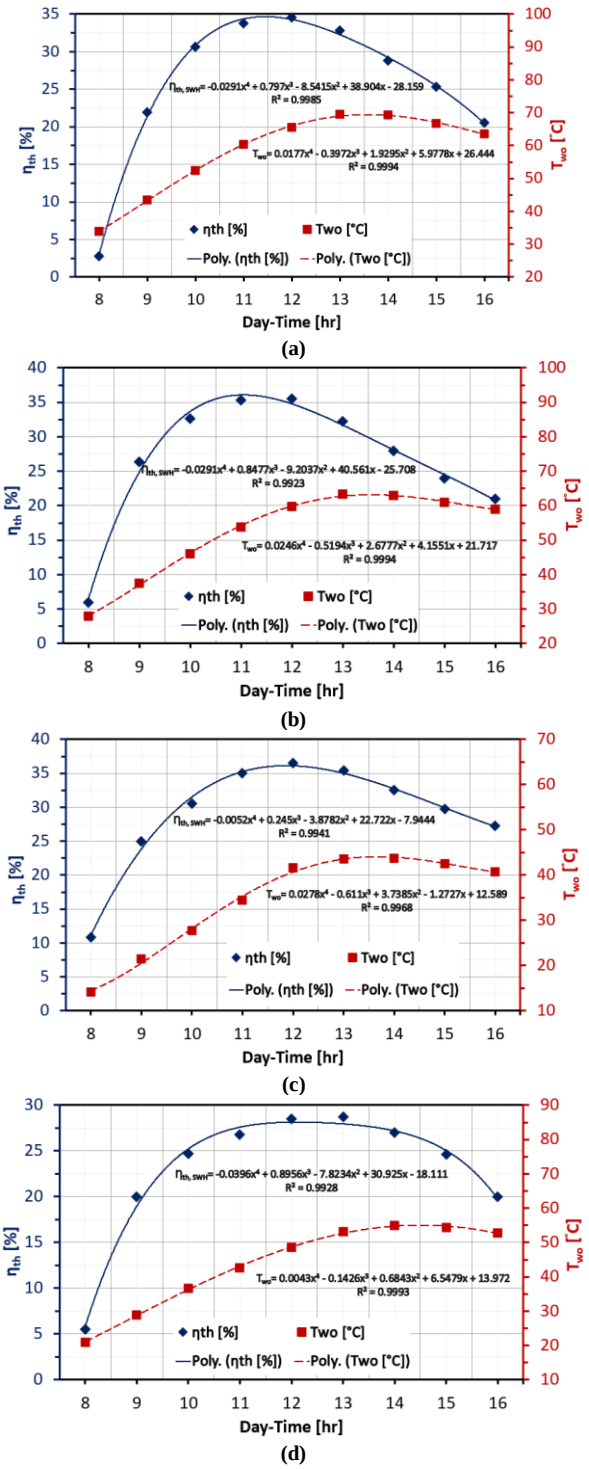


**Fig. 9.** Fluctuation of the SWH thermal efficiency ($\eta_{th}$) and the output collector temperature ($T_{wo}$) across the test period for (a) June 21, 2021, (b) September 23, 2021, (c) December 21, 2021, and (d) March 22, 2022.

Finally, concerning the original configuration of the present integrated system, the recorded temperatures show a largely appropriate and suitable range. The recorded water temperatures, as shown in Table 3, confirm that the SWH under investigation is operating effectively. In experimentations 1 and 2, which were conducted in the summer and autumn, the average instantaneous efficiency or daily efficiency was about 28.5% and 29.5%, respectively. The average surrounding climate, with sun insolation surpassing 620 W/m$^2$ and average ambient temperature exceeding 30°C, is what produced these results.

Because of the drop in sun insolation, which in trial no. 4 or spring reached about 575 W/m$^2$, the average instantaneous efficiency was impacted and reached 26.5% (Table 3). The average instantaneous efficiency was the highest at 31.5% despite the decrease in sun insolation, which reached approximately 415 W/m$^2$ in test no. 3, or winter. This phenomenon might be attributed to factors such as the inclination angle of the tubular collector, solar parameters like altitude and azimuth, or the notably low water temperatures and their ability to maximize heat absorption.

**Table 3.** A summary of the average results obtained from the SWH tests.

| Test date | Test season | $I_{s,avg}$ (W/m$^2$) | $T_{amb,avg}$ (°C) | $T_{wi,avg}$ (°C) | $T_{wo,avg}$ (°C) | $\eta_{th,avg}$ (%) |
|---|---|---|---|---|---|---|
| June 21, 2021 | Summer | 788 | 39 | 47 | 58.5 | 28.6 |
| September 23, 2021 | Autumn | 621 | 33 | 43.5 | 52.5 | 29.5 |
| December 21, 2021 | Winter | 414 | 20 | 28 | 34.5 | 31.5 |
| March 22, 2022 | Spring | 576 | 27 | 36.5 | 44 | 26.6 |

## 4 Conclusions and Future Works

The creatively designed system combines the idea of a solar water heater with a solar light tube system; the difference is that the plate is now tubular rather than flat. Lower production costs and space needs are the outcomes of this combination. To fully assess the system's performance, the thermal performance of the current solar heater has undergone extensive experimental testing and analysis throughout a variety of seasons. The following important outcomes can be drawn from this research:

- The ratio $\Delta T_w/I_s$ was shown to grow with an increase in solar radiation and change in water temperature. This, in turn, led to an increase in the efficiency of the tubular collector, which reached its peak before progressively declining throughout the year seasons.
- A successful performance is shown by the greatest instantaneous efficiency of around 36% and the highest temperature for water of about 70°C, respectively.
- During the trials, the suggested solar water heater's maximum daily thermal efficiency was about 31%.
- Ultimately, from the all results obtained, the proposed integration strategy presents a viable and effective solution to address Egypt's daytime power interruption challenges by harnessing solar energy for electricity saving.

Recommendations for future work can be summarized as:

- The coil number of turns in the SWH should be numerous and cover most of the absorber area, as it directly affects the solar heater efficiency.
- Using a storage material inside the SWH storage tank to increase the productivity during the night hours.
- To facilitate precise control and maintenance of water temperature during late daytime hours and at night period, the utilization of a variable-speed rotary pump, accompanied by two solenoid-valves and a controller, is imperative in the SWH.
- An embedded ventilation fan powered through the PV panel and battery could be added to the SLP to allow air circulation indoors.

**Nomenclature**

*Latin alphabet*

| | |
|---|---|
| A | Area, [m$^2$] |
| $Al_2O_3$ | Aluminium oxide |
| $CO_2$ | Carbon dioxide |
| $C_p$ | Specific heat, [J. kg$^{-1}$. °C$^{-1}$] |
| $I_s$ | Solar insolation, [W. m$^{-2}$] |
| k | Thermal conductivity, [W. m$^{-1}$. °C$^{-1}$] |
| $\dot{m}$ | Mass flow rate, [kg. s$^{-1}$] |
| Q | Thermal energy transfer, [W] |
| Q | Volume flow rate, [m$^3$. s$^{-1}$] |
| T | Temperature, [°C] |

*Greek alphabet*

| | |
|---|---|
| $\eta_{th, ins}$ | Instantaneous efficiency [%] |
| Θ | Incidence angle, [deg] |
| ρ | Density, [kg. m$^{-3}$] |

*Subscripts*

| | |
|---|---|
| abs | Absorber |
| amb | Ambient |
| avg | Average |
| i | Input |
| o | Output |
| s | Solar |
| w | Water |

*Abbreviations*

| | |
|---|---|
| FPC | Flat Plate Collector |
| PCM | Phase Change Material |
| SLP | Solar Light Pipe |
| SWH | Solar Water Heater |
| TPC | Tubular Plate Collector |
| TT | Twisted Tape |

## References


[1] ELECTRICITY INFORMATION: OVERVIEW (2023) edition, available from; https://www.iea.org/reports/electricity-2023.

[2] Global share of electricity generation by source (2023), IEA, Paris, available from; https://www.iea.org/data-and-statistics/charts/global-share-of-electricitygeneration-2023.

[3] Egyptian Electricity Holding Company - Annual Reports; http://www.moee.gov.eg/englishnew/report.aspx.

[4] L. Cozzi, et al. "World energy outlook 2021." International Energy Agency: Paris, France (2021): 1-461. https://gotcp.net/wp-content/uploads/2021/10/WEO2021_Launch_Presentation-1.pdf.

[5] A.H. Mohammed, M. Attalla, and A.N. Shmroukh. "Performance enhancement of single-slope solar still using phase change materials." Environmental Science and Pollution Research 28.14 (2021): 17098-17108. https://doi.org/10.1007/s11356-020-12096-x.

[6] A.H. Mohammed, M. Attalla, and A.N. Shmroukh. "Comparative study on the performance of solar still equipped with local clay as an energy storage material." Environmental Science and Pollution Research 29.49 (2022): 74998-75012. https://doi.org/10.1007/s11356-022-21095-z.

[7] A.H. Mohammed, A.N. Shmroukh, and M. Attalla. "Optimum seawater depth in modified solar still using vertical flax porous media." International Journal of Applied Energy Systems 2.1 (2020): 6-10. https://ijaes.journals.ekb.eg/article_169933.html.

[8] M.E. El-saggan, et al. "A Review of the Evolution of Daylighting Applications and Systems Over Time for Green Buildings." International Journal of Applied Energy Systems 5.2 (2023): 31-47. https://doi.org/10.21608/ijaes.2023.187498.1016.

[9] B. Yildiz, et al. "Analysis of electricity consumption and thermal storage of domestic electric water heating systems to utilize excess PV generation." Energy 235 (2021): 121325. https://doi.org/10.1016/j.energy.2021.121325.

[10] A.G. Gaglia, et al. "Energy performance of European residential buildings: Energy use, technical and environmental characteristics of the Greek residential sector–energy conservation and $CO_2$ reduction." Energy and Buildings 183 (2019): 86-104. https://doi.org/10.1016/j.enbuild.2018.10.042.

[11] M. Tewar, et al. "Reimagining India's urban future: A framework for securing high-growth, low-carbon, climate-resilient urban development in India." (2015). https://www.academia.edu/download/55389392/Urban_Future_Working_Paper_306.pdf.

[12] A.H. Mohammed, et al. "Performance evaluation and optimization of solar dish concentrator in the upper Egypt region." Environmental Progress & Sustainable Energy (2023): e14325. https://doi.org/10.1002/ep.14325.

[13] A.H. Mohammed, et al. "Active solar still with solar concentrating systems, Review." Journal of Thermal Analysis and Calorimetry 148.17 (2023): 8777-8792. https://doi.org/10.1007/s10973-023-12285-z.

[14] R.B. Slama. "Experimentation of a plane solar integrated collector storage water heater." Energy and Power Engineering 4.02 (2012): 67-76. DOI:10.4236/epe.2012.42010.

[15] B. Hellstrom, et al. "The impact of optical and thermal properties on the performance of flat plate solar collectors." Renewable Energy 28.3 (2003): 331-344. https://doi.org/10.1016/S0960-1481(02)00040-X.

[16] S. Föste, et al. "Flat plate collectors with thermochromic absorber coatings to reduce loads during stagnation." Energy Procedia 91 (2016): 42-48. https://doi.org/10.1016/j.egypro.2016.06.169.

[17] J. Jyothi, et al. "Design and fabrication of spectrally selective TiAlC/TiAlCN/TiAlSiCN/TiAlSiCO/TiAlSiO tandem absorber for high-temperature solar thermal power applications." Solar energy materials and solar cells 140 (2015): 209-216. https://doi.org/10.1016/j.solmat.2015.04.018.

[18] H.C. Barshilia, N. Selvakumar, and K. S. Rajam. "Thermal stability of TiAlN/ TiAlON/ $Si_3N_4$ tandem absorbers prepared by reactive direct current magnetron sputtering." Journal of Vacuum Science & Technology A 25.2 (2007): 383-390. https://doi.org/10.1116/1.2699425.

[19] K.K. Matrawy and I. Farkas. "Comparison study for three types of solar collectors for water heating." Energy conversion and management 38.9 (1997): 861-869. https://doi.org/10.1016/S0196-8904(96)00089-1.

[20] H.C. Hottel and B.B. Woertz. "The performance of flat-plate solar-heat collectors." Transactions of the American Society of Mechanical Engineers 64.2 (1942): 91-103. https://doi.org/10.1115/1.4018980.

[21] M. Smyth, P. C. Eames, and B. Norton. "Integrated collector storage solar water heaters." Renewable and Sustainable Energy Reviews 10.6 (2006): 503-538. https://doi.org/10.1016/j.rser.2004.11.001.

[22] A.S. Kalogirou. "Solar thermal collectors and applications." Progress in energy and combustion science 30.3 (2004): 231-295. https://doi.org/10.1016/j.pecs.2004.02.001.

[23] M.M. Salama, et al. "Experimental investigation on a thermochemical seasonal sorption energy storage battery utilizing $MgSO_4$-$H_2O$." Environmental Science and Pollution Research 30.43 (2023): 98502-98525. https://doi.org/10.1007/s11356-023-28875-1.

[24] F. Motte, et al. "Numerical study of PCM integration impact on overall performances of a highly building-integrated solar collector." Renewable Energy 137 (2019): 10-19. https://doi.org/10.1016/j.renene.2017.12.067.

[25] J. Assadeg, et al. "Energetic and exergetic analysis of a new double pass solar air collector with fins and phase change material." Solar Energy 226 (2021): 260-271. https://doi.org/10.1016/j.solener.2021.08.056.

[26] M.A. Fazilati and A.A. Alemrajabi. "Phase change material for enhancing solar water heater, an experimental approach." Energy conversion and management 71 (2013): 138-145. https://doi.org/10.1016/j.enconman.2013.03.034.

[27] W. Wu, et al. "Experimental study on the performance of a novel solar water heating system with and without PCM." Solar Energy 171 (2018): 604-612. https://doi.org/10.1016/j.solener.2018.07.005.

[28] H.H. Al-Kayiem and S.C. Lin. "Performance evaluation of a solar water heater integrated with a PCM nanocomposite TES at various inclinations." Solar Energy 109 (2014): 82-92. https://doi.org/10.1016/j.solener.2014.08.0 21.

[29] G. Murali, K. Mayilsamy, and T. V. Arjunan. "An experimental study of PCM-incorporated thermosyphon solar water heating system." International Journal of Green Energy 12.9 (2015): 978-986. https://doi.org/10.1080/15435075.2014.888663.

[30] S. Bouadila, et al. "Enhancement of latent heat storage in a rectangular cavity: solar water heater case study." Energy conversion and management 78 (2014): 904-912. https://doi.org/10.1016/j.enconman.2013.07.094.

[31] P.M. Kumar and K. Mylsamy. "Experimental investigation of solar water heater integrated with a nanocomposite phase change material: Energetic and exergetic approach." Journal of Thermal Analysis and Calorimetry 136 (2019): 121-132.

https://doi.org/10.1007/s10973-018-7937-9.
[32] A.S. Manirathnam, et al. “Experimental analysis on solar water heater integrated with Nano composite phase change material (SCi and CuO).” Materials Today: Proceedings 37 (2021): 232-240. https://doi.org/10.1016/j.matpr.2020.05.093.
[33] U. Stritih. “An experimental study of enhanced heat transfer in rectangular PCM thermal storage.” International Journal of Heat and Mass Transfer 47.12-13 (2004): 2841-2847. https://doi.org/10.1016/j.ijheatmasstransfer.2004.02.001.
[34] S. Canbazoğlu, et al. “Enhancement of solar thermal energy storage performance using sodium thiosulfate pentahydrate of a conventional solar water-heating system.” Energy and buildings 37.3 (2005): 235-242. https://doi.org/10.1016/j.enbuild.2004.06.016.
[35] B. Li and X. Zhai. “Experimental investigation and theoretical analysis on a mid-temperature solar collector/storage system with composite PCM.” Applied Thermal Engineering 124 (2017): 34-43. https://doi.org/10.1016/j.applthermaleng.2017.06.002.
[36] M. Kenisarin, et al. “Enhancing thermal conductivity of paraffin wax 53–57°C using expanded graphite.” Solar Energy Materials and Solar Cells 200 (2019): 110026. https://doi.org/10.1016/j.solmat.2019.110026.
[37] M. Mirzaei, S.M.S. Hosseini, and A.M.M. Kashkooli. “Assessment of $Al_2O_3$ nanoparticles for the optimal operation of the flat plate solar collector.” Applied Thermal Engineering 134 (2018): 68-77. https://doi.org/10.1016/j.applthermaleng.2018.01.104.
[38] M.N. Metwally, H.Z. Abou-Ziyan, and A.M. El-Leathy. “Performance of advanced corrugated-duct solar air collector compared with five conventional designs.” Renewable Energy 10.4 (1997): 519-537. https://doi.org/10.1016/S0960-1481(96)00043-2.
[39] A. Abene, et al. “Study of a solar air flat plate collector: use of obstacles and application for the drying of grape. ” Journal of food engineering 65.1 (2004): 15-22. https://doi.org/10.1016/j.jfoodeng.2003.11.002.
[40] A. Kumar and B.N. Prasad. “Investigation of twisted tape inserted solar water heaters—heat transfer, friction factor and thermal performance results.” Renewable energy 19.3 (2000): 379-398. https://doi.org/10.1016/S0960-1481(99)00061-0.
[41] G. Puthilibai, et al. “Study on the impact of twisted tapes on the water temperature enhancement in solar water heater.” Materials Today: Proceedings 62 (2022): 5114-5118. https://doi.org/10.1016/j.matpr.2022.02.459.
[42] J. Twidell. “Renewable energy resources.” Routledge (2021).
[43] S. Klein, et al. “Computers in the design of solar energy systems.” Energy 4.4 (1979): 483–501. https://doi.org/10.1016/0360-5442(79)90078-1.
[44] J.A. Duffie and W.A. Beckman. “Solar Engineering of Thermal Processes.” John Wiley & Sons, 4th edition (2013). http://ndl.ethernet.edu.et/bitstream/123456789/87795/1/Solar%20Engineering%20of%20Thermal%20Processes%2C%204th%20Edition%20-%20GearTeam.pdf.